NORSAR

NORSAR Scientific Report No. 1-2011

Semiannual Technical Summary

1 July - 31 December 2010

Frode Ringdal (ed.)

Kjeller, February 2011

6.4 Test of new hybrid seismometers at NORSAR

6.4.1 Introduction

In the framework of the recapitalization of the NORSAR arrays NOA and ARCES (primary stations PS27 and PS28, respectively) and a potential modernization of the SPITS array (auxiliary station AS72) we wish to install new digitizers and sensors. One of our goals was to specify one sensor type suitable for all our arrays. Having a uniform sensor at all sites will simplify maintenance and data processing as well as improve the operational readiness, because of the interchangeability of spare parts.

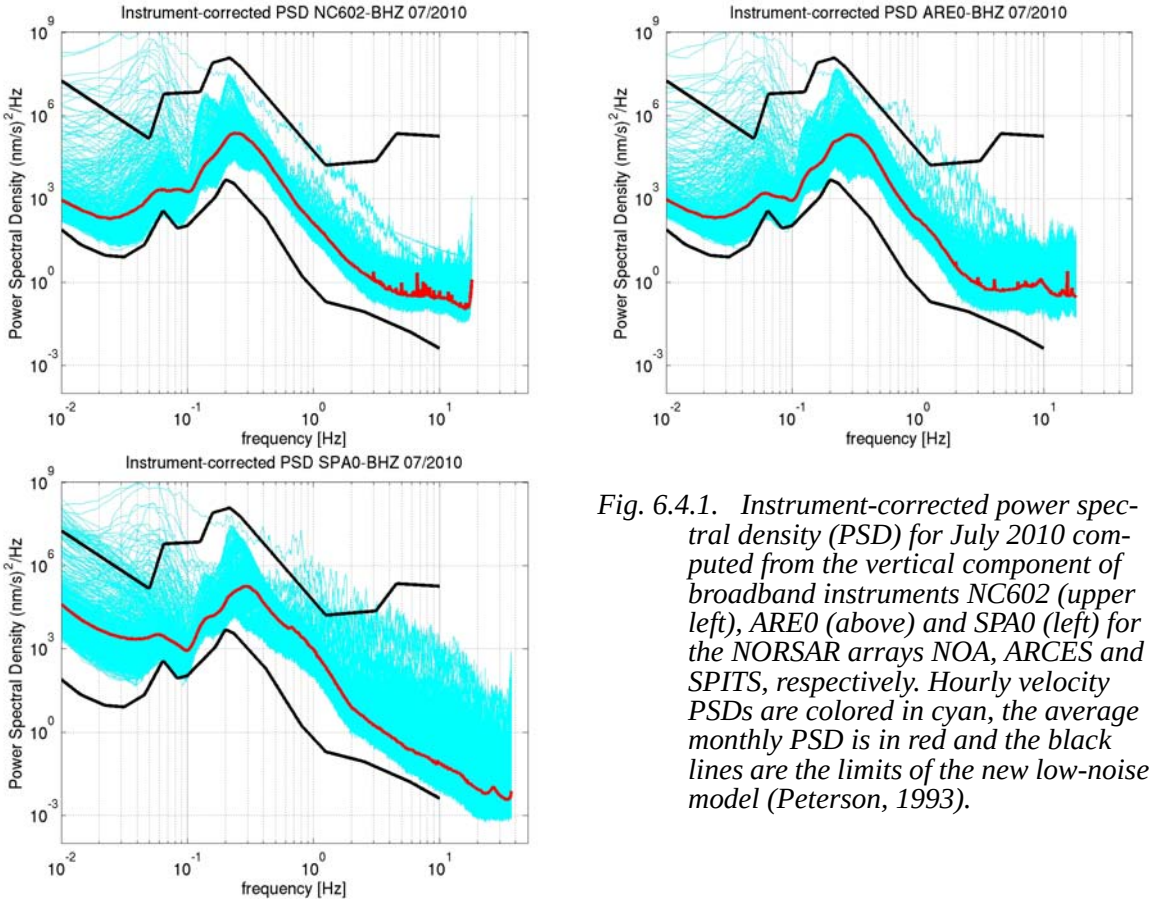

Fig. 6.4.1. Instrument-corrected power spectral density (PSD) for July 2010 computed from the vertical component of broadband instruments NC602 (upper left), ARE0 (above) and SPA0 (left) for the NORSAR arrays NOA, ARCES and SPITS, respectively. Hourly velocity PSDs are colored in cyan, the average monthly PSD is in red and the black lines are the limits of the new low-noise model (Peterson, 1993).

Figure 6.4.1 gives an overview on conditions for three sites NC602, ARE0 and SPA0 (broadband sites in NOA, ARCES and SPITS, respectively) for July 2010. For each hour we computed the power spectral density for the vertical components, corrected for instrument response and plotted the 744 curves on top of each other. The red curve is the average PSD for the month and the black lines are the bounds of the Peterson (1993) new low-noise model. We did not sort out time periods that contained seismic events, which contributes to the broad variation in the set of curves and causes a certain bias of the average curve. However, we clearly can determine the lower noise limit for the sites. For NOA and ARCES the ambient noise during quiet conditions is close to or even touches the low-noise Peterson model for frequencies below 0.2 Hz. At SPITS we have higher noise-levels for very low frequencies (<0.05 Hz), but in the high-fre-

quency range (> 4 Hz) the site is very quiet due to the absence of any industrial and man-made noise.

Figure 6.4.2 shows the transfer function of seismic sensors (digitizer response/gain included) in use at the NORSAR arrays. Most of the instruments are proportional to velocity (Guralp 3T NOA, Guralp 3T ARCES, STS2 NOA test bed, STS2 JMIC, Teledyne T20171 (for f < 1 Hz)), but two of them (Guralp 3T SPITS and KS5400) are proportional to acceleration. In order to decide on a new sensor type we were taking into account the ambient noise conditions and the experiences with our existing systems. In our opinion the current system at SPITS has too high gain for high-frequencies. At ARCES the sensor gain is fine for high frequencies, but it is too high for frequencies below 1 Hz. The KS5400 at NOA lacks sensitivity for very low frequencies and for frequencies higher than 10 Hz.

Eventually we decided to go for a seismic sensor with a newly designed hybrid response. We specified the desired shape and Guralp Systems designed and fabricated the sensor. The sensor has a sensitivity of 2x20 000 V/m/s at 5 Hz and it is proportional to velocity for 1/360 Hz - 1/3 Hz, proportional to acceleration for 1/3 Hz - 2 Hz and again proportional to velocity for 2 Hz - 50 Hz. The Guralp 3T Hybrid response is shown in Figure 6.4.2 It is less sensitive than the Guralp 3T ARCES instrument at lower frequencies, it fits the Teledyne T20171, the KS5400 and the Guralp 3T SPITS at about 5 Hz and it has lower sensitivity than the Guralp 3T SPITS at high frequencies.

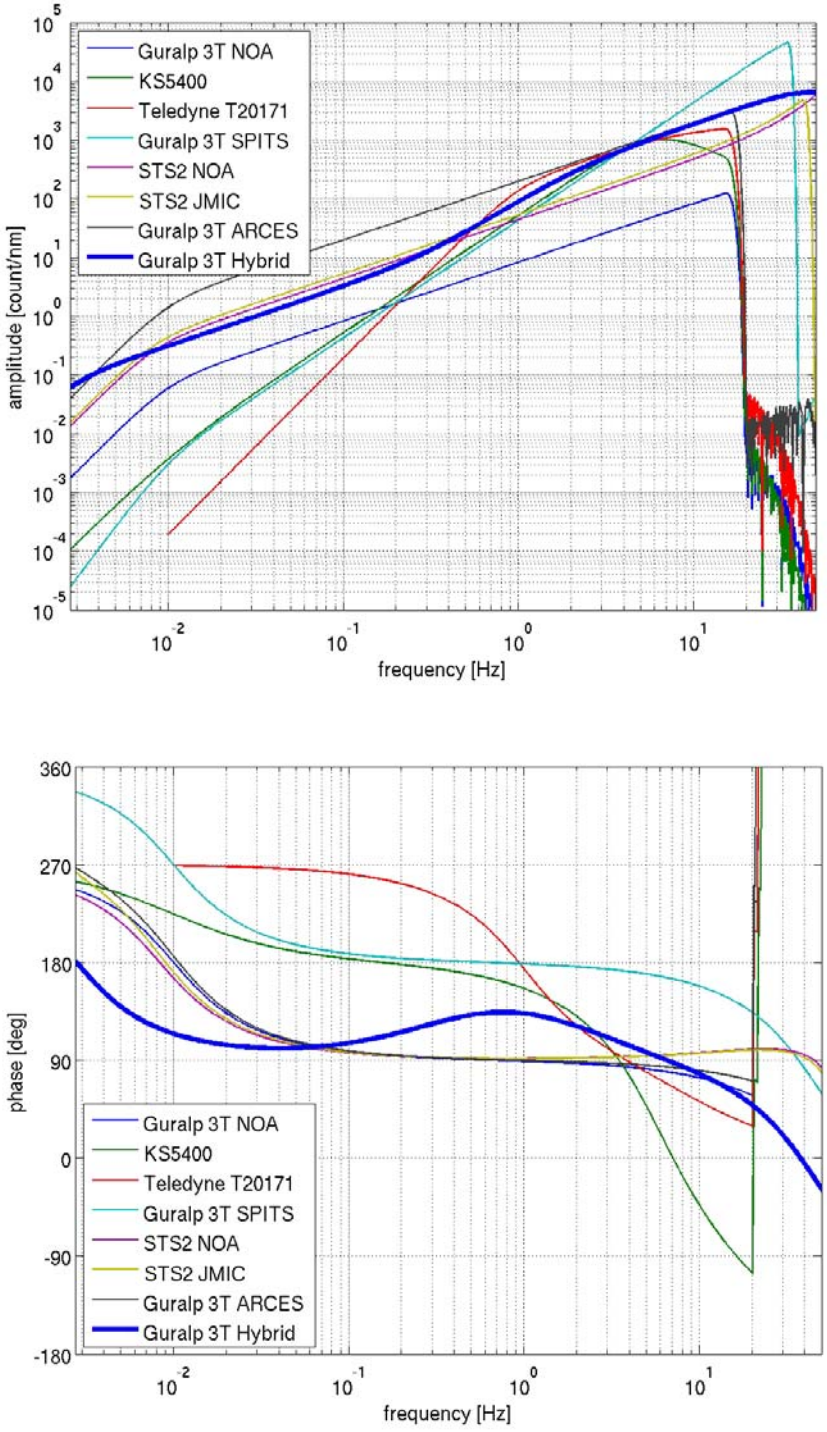

Fig. 6.4.2. Transfer functions for different sensors in use at the NORSAR arrays. Top: Amplitude response in units of counts/nanometer (site specific digitizer response/gain included). Bottom: Phase response.

6.4.2 Instrument tests

In the beginning of 2010 NORSAR received two prototypes of the new hybrid sensor. The sensors had the same instrument response but different sensitivity, i.e. 2x15000 V/m/s and 2x60000 V/m/s. Besides problems with reversed polarity we found undesirable high frequency noise bumps around 35-50 Hz. At the low frequency end we found incoherence between the sensors part of which could be associated with thermic convection and noise induced by the very stiff seismometer cables. In the following we discuss the tests on the second batch of instruments (5 Guralp 3T hybrid with 2x20000 V/m/s)

NORSAR has a test facility at the site NC602 of the NOA array. Figure 6.4.3 shows the central building at the site. About 20 m to the right of the building is a subsurface bunker that houses the IMS short-period Teledyne and Guralp instrument. The spacious bunker has three seismometer pits out of which two have been used for testing purposes. Figure 6.4.3 (bottom left) shows one of the pits with 7 instruments covered by thermal insulation tubes. The right side of Figure 6.4.3 shows an opened Guralp hybrid 3T.

Fig. 6.4.3. Top left: Central building of the NORSAR test facility. The subsurface vault containing the broadband site NC602 and the test instruments is to the right of the building. Bottom left: One out of three pits in the vault with thermically insulated Guralp instruments. Right: An open Guralp 3T hybrid instrument.

A main goal of the tests was to investigate the noise level of the sensors and the coherency between the instruments. The left hand side of Figure 6.4.4 shows PSDs for September 2010 for the IMS broadband sensor at NC602. Based on these types of displays (http:// www.norsardata.no/NDC/spectraplot/) we have been searching for quiet periods to analyze the test data. The right hand side of Figure 6.4.4 shows an 8-hour time window of raw data (Z, East and North component from top to bottom) recorded with 5 hybrid instruments located in one of the seismometer pits.

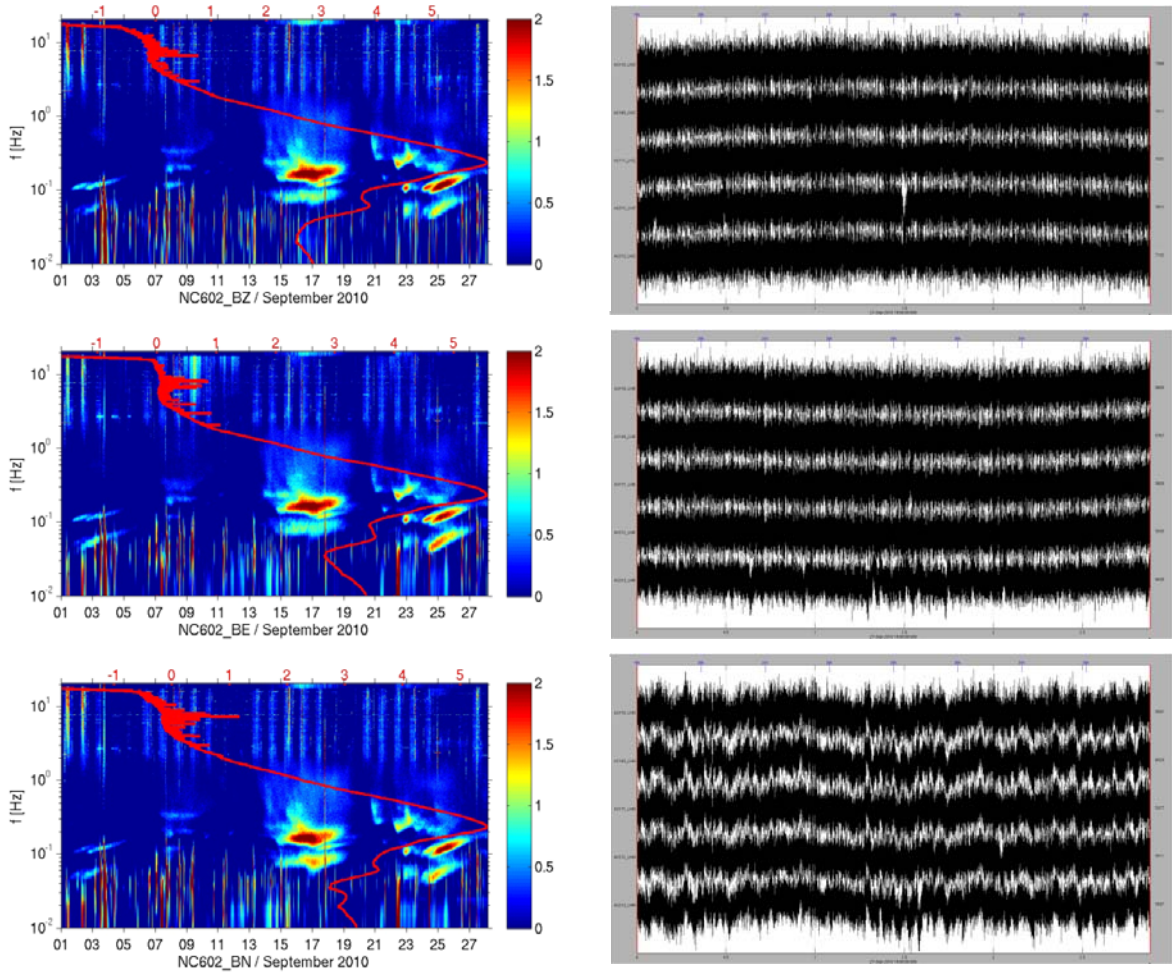

Fig. 6.4.4. Left column: Power spectral density (PSD) for the broadband instrument NC602 (Z, East and North component, raw data) for September 2010. The red curve shows the average PSD of the entire month and residuals from the average are color-coded. Right: Waveforms recorded with 5 colocated hybrid seismometers (Z, East and North component from top to bottom) for an eight-hour time window (start 27.09.2010 19:00). In each panel the traces from top to bottom correspond to digitizer/instrument A2118/T36307, A2149/T35728, A2171/T36340, A2212/T36344, and A2213/T36309, respectively.

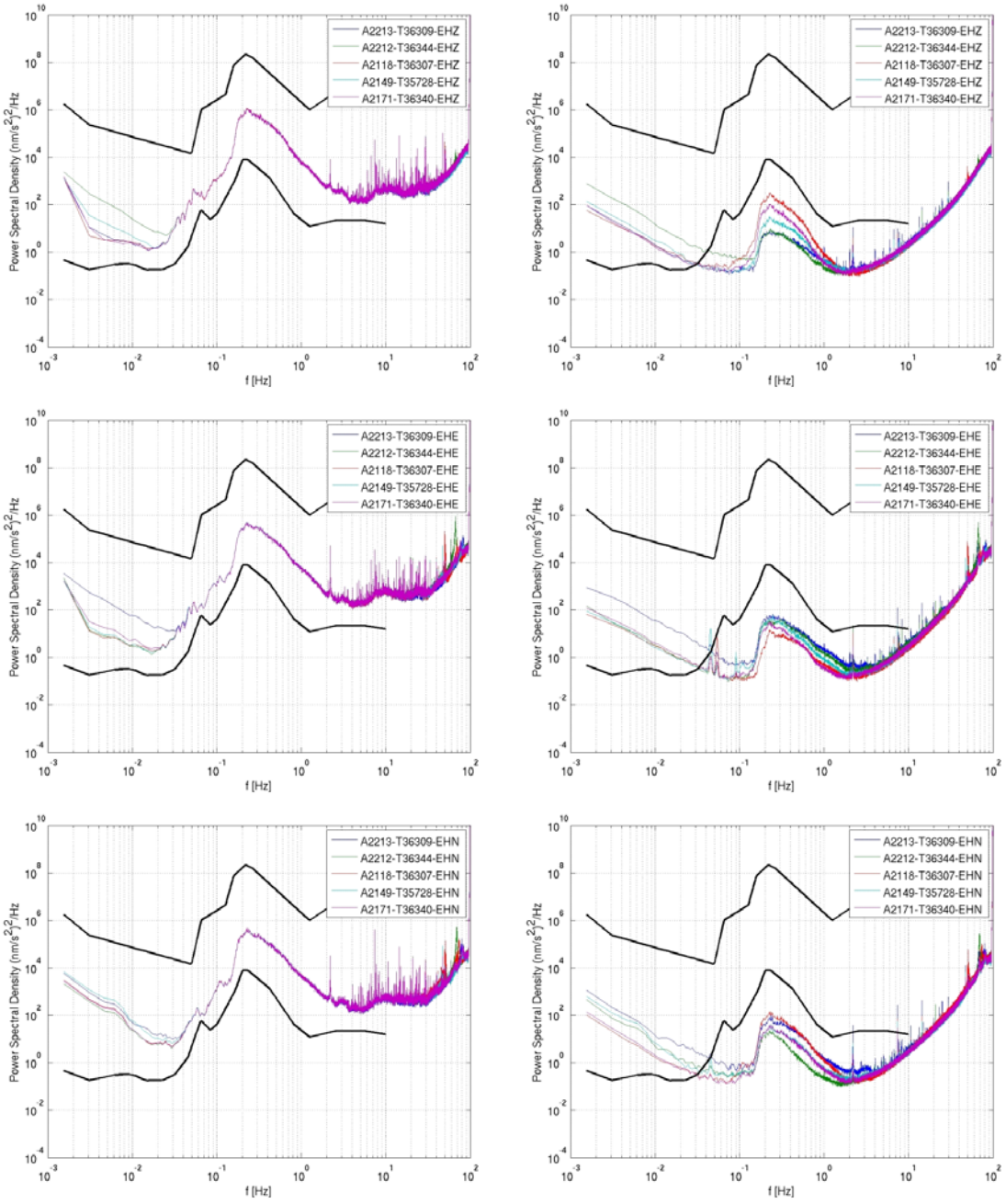

Fig. 6.4.5. Left: Instrument-corrected PSD (Z-, East and North component from top to bottom) computed for the eight-hour seismograms shown in Figure 6.4.1 We used 600 s windows with 300 s overlap and the PSD is for acceleration, i.e. in units of $(nm/s^2)^2$/Hz. Right: Instrument-corrected PSD of incoherent traces, i.e. we subtracted the average waveform and computed the PSD of the residual.

From the raw data in Figure 6.4.4 (right) we computed the power spectral density using Welch's method (1967) with time window lengths of 600 s and 300 s overlap. Figure 6.4.5 (left) shows the resulting PSDs corrected for the nominal acceleration instrument response. The PSDs for the different instruments coincide very well for frequencies above 0.03 Hz. All spectra have the identical noise peaks in the frequency range from about 2-50 Hz. These noise peaks are not related to the hybrid sensors (we see them also with other instruments at the site),

but are manmade (e.g. turbine of hydro-power plants) and electrical noise. For low-frequencies (< 0.03 Hz we see that some of the sensors deviate. This is partly due to settling effects or burps of the sensor. At very high frequencies (> 50 Hz) the spectra for the horizontal components exhibit differences, but this is outside of the frequency range of interest.

Since the instruments are co-located they should record the very same input signals (ambient seismic signals) and should produce the very same output. Differences in the output can be interpreted as instrument noise (intrinsic, but also settling events etc.). One approach to estimate the instrument noise is to compute an average output trace from all 5 instruments, subtract the average trace from the single recordings and compute the PSD of the residual traces. The results are displayed in Figure 6.4.5 (right column). The PSDs of the instrument noise is below the low-noise Peterson model for frequencies above 0.03 - 0.04 Hz. The higher instrument noise in the frequency range of the microseisms could be partly an artifact of the computational method, but it is anyway well below the low-noise model.

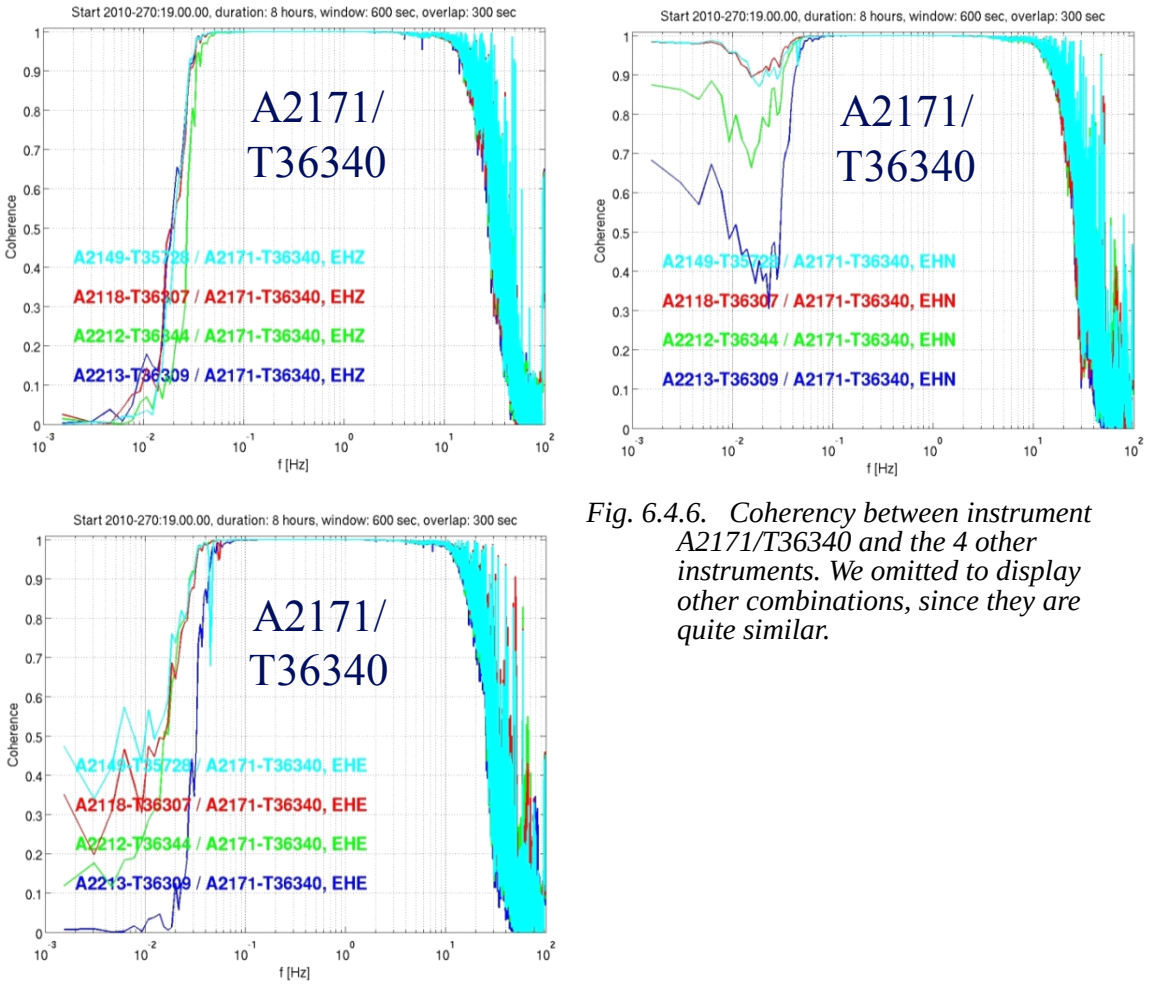

Fig. 6.4.6. Coherency between instrument A2171/T36340 and the 4 other instruments. We omitted to display other combinations, since they are quite similar.

Power spectral density is one way to compare instrument performance, but it does not give information on the signal coherency between the different instrument outputs. The coherency is defined as $C=|P_{12}|^2/(P_{11}P_{22})$, where P_{11}, P_{22} and P_{12} are the power spectral densities (PSD) for system 1 and 2 and cross-spectral density between the systems outputs, respectively (e.g.

Kay 1988). Representative for all results Figure 6.4.6 shows the coherency between A2171/ T36340 and the other 4 instruments. Coherency should be 1 for perfect trace alignment and this can be observed over a broad frequency range. At the low frequency end it starts to decrease at around 0.03 Hz (vertical components) and 0.04 Hz (horizontal components); at the high frequency end it starts to detoriate at 10 - 20 Hz. The coherency for the North component recovers again for low frequencies, which is an indication that there was coherent ambient seismic noise polarized in N-S direction. At that occasion it is important to mention that we observe nearly perfect coherence over the entire frequency range in the presence of a seismic event.

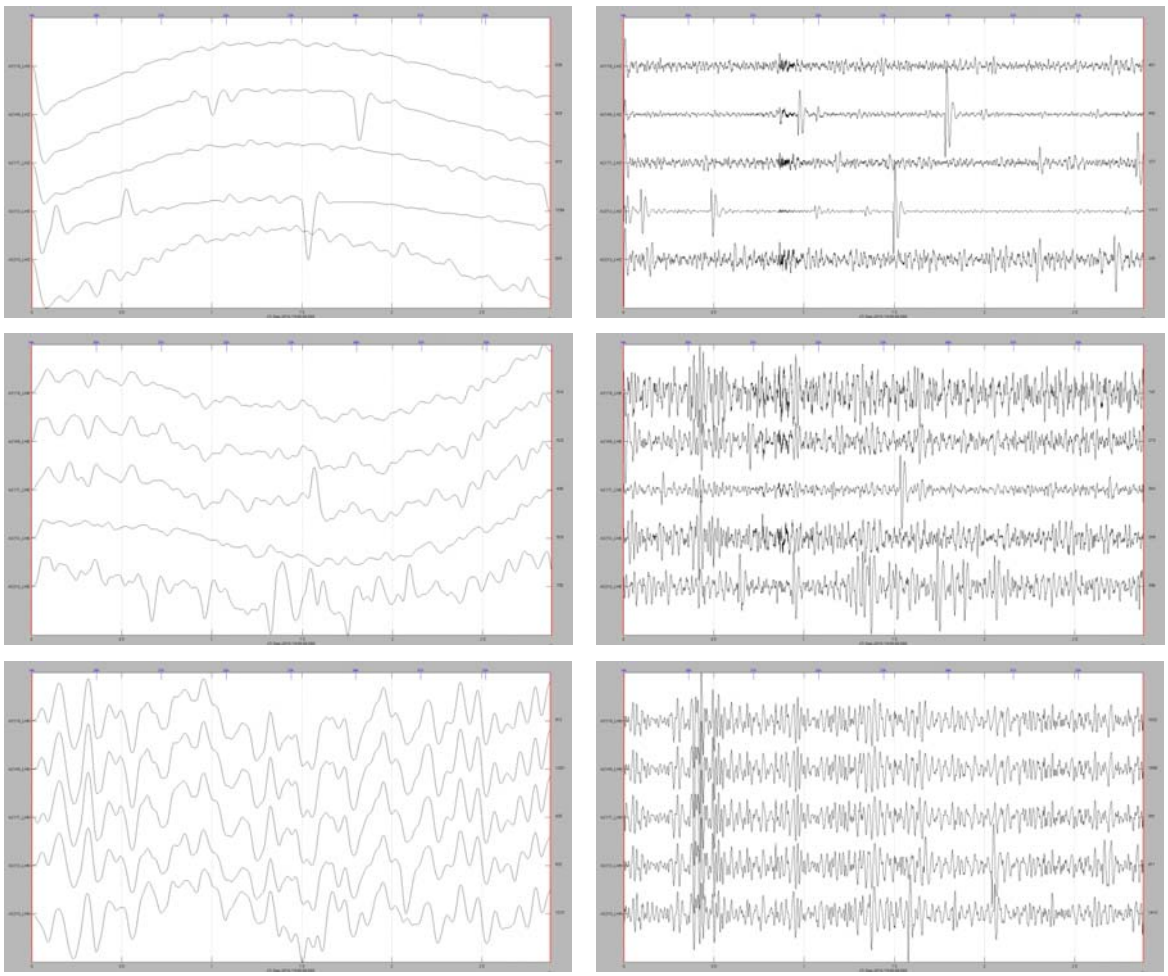

Fig. 6.4.7. Waveform comparison between the 5 hybrid instruments for different frequency bands. Left column: 8-hour time window and 1000 s low-pass. Right column: 8-hour time window and bandpass between 360 s- 50 s. The Z, East and North components are shown in the top, middle and lower panel, respectively. The trace order is the same as in Figure 6.4.4 (left).

A third way to compare the instruments is to compare directly the waveforms for different frequency bands. This is done in Figure 6.4.7 - Figure 6.4.9 For very low frequencies > 0.001 Hz (Figure 6.4.7 left column) one can see the earth tides on the Z and East component (confirmed also by observations with a Streckeisen STS2 at the test site); in addition, the vertical component also show settling events. On the North component we find coherent seismic signals with about twice the earth tide amplitudes. We do not know the reason for the of the relatively strong and coherent signals on the N components, but it is certainly not an instrumental feature

or caused by thermal convection, since we also see them on the STS2 in the neighbor pit. Figure 6.4.7 (right column) displays the waveforms for a filter band between 360 s - 50 s.We see again good coherency of the North-components due to the high amplitudes of the ambient seismic signal. The East and vertical components show weak coherency. The poor coherency of the vertical components is mainly caused by a number of settling events, which will cease in time.

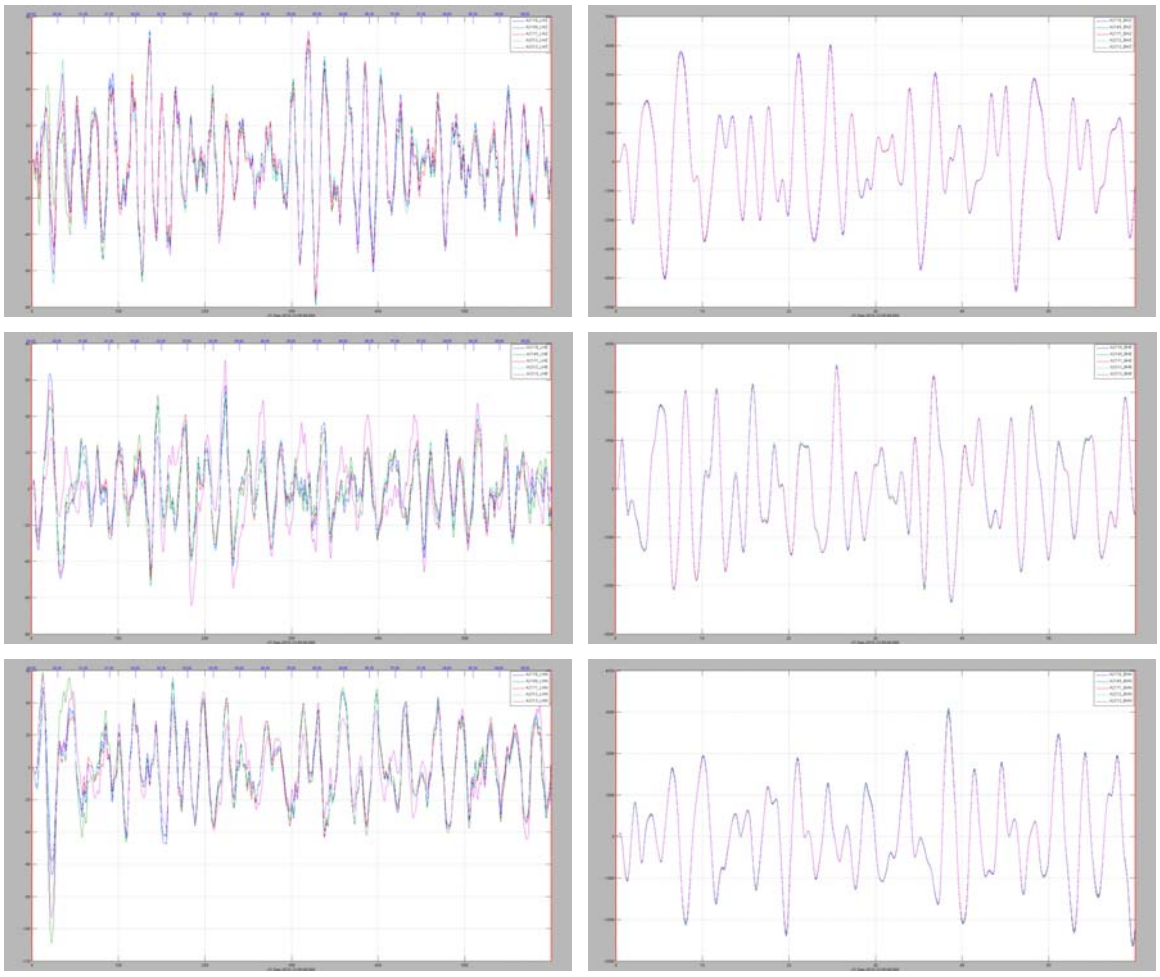

Fig. 6.4.8. Same as Figure 6.4.7, but for shorter time windows and higher frequency bands. The waveforms are now overlaid for better comparison. Left: 10-minute time window and bandpass between 0.02 Hz - 0.05 Hz. Right: 1-minute time window and bandpass between 0.05 Hz - 1 Hz.

Figure 6.4.8 shows the trace overlaid for better comparison. For a bandpass between 0.02 Hz - 0.05 Hz (left column) we see deviations between the horizontal components and very minute differences of between the vertical traces. For a bandpass 0.05 Hz - 1 Hz (Figure 6.4.8 right column) and 1 Hz - 20 Hz (Figure 6.4.9 left column) we observe perfect alignment of all traces. In the very high frequency band 20 Hz - 40 Hz (Figure 6.4.9 right column) the similarity between the traces starts to decrease again. The phase coherency is still ok for most of the wavelets, but we can observe differences in the amplitudes.

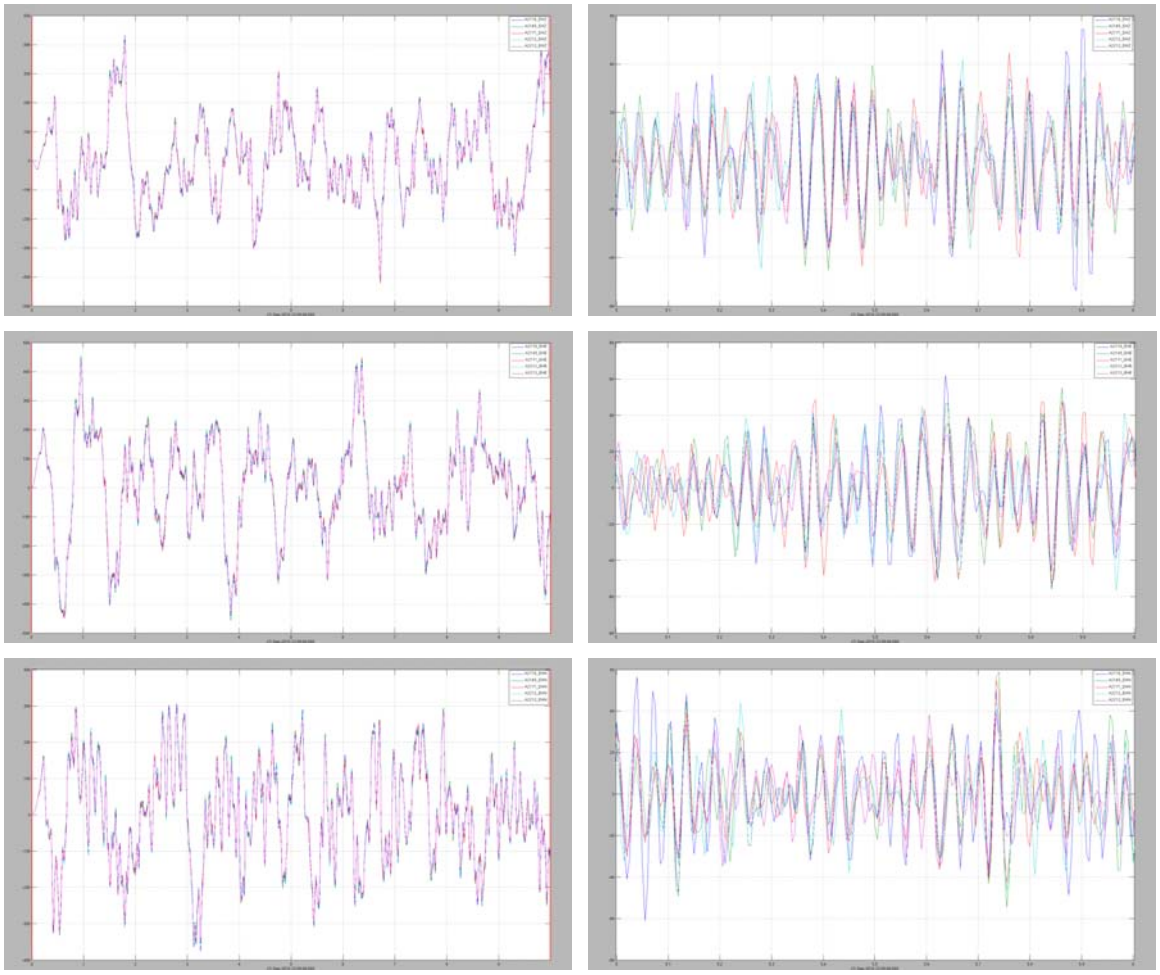

Fig. 6.4.9. Same as Figure 6.4.8, but for shorter time windows and higher frequency bands: Left: 10-second time window and bandpass between 1 Hz - 20 Hz. Right: 1-second time window and bandpass between 20 Hz - 40 Hz.

6.4.3 Conclusions

In the framework of the recapitalization of the NORSAR arrays we intend to install new seismic sensors with a hybrid response function. The transfer function of the instruments was designed to be suitable for the ambient noise conditions of our sites and to deliver similar or higher data quality than the existing systems are doing. The instrument noise of the new hybrid sensors is below the Peterson model for frequencies above 0.03 Hz. The coherency is very good (> 0.9) for frequencies between 0.03 Hz and 20 Hz under quiet ambient noise conditions. From direct waveform comparisons we can conclude that we can expand these frequency limits (especially in the high-frequency end) for practical applications, because the waveform similarity is still good.

6.4.4 References

Kay, S. M. (1988) Modern Spectral Estimation. Englewood Cliffs, NJ: Prentice-Hall, 1988. pp.453-455.

Peterson, J. (1993). Observations and modeling of seismic background noise. USGS Open-File Report 93-322.

Welch, P. D. (1967). The Use of Fast Fourier Transform for the Estimation of Power Spectra: A Method Based on Time Averaging Over Short, Modified Periodograms", IEEE Transactions on Audio Electroacoustics, Volume AU-15 (June 1967), pages 70–73.

Michael Roth
Jan Fyen
Paul W. Larsen
Johannes Schweitzer